

**MOLECULAR DYNAMICS STUDIES OF THE
ANNEALING OF CARBON PEAPODS**

LEE THONG YAN

UNIVERSITI SAINS MALAYSIA

2018

**MOLECULAR DYNAMICS STUDIES OF THE
ANNEALING OF CARBON PEAPODS**

by

LEE THONG YAN

**Thesis submitted in fulfillment of the requirements
for the degree of
Doctor of Philosophy**

August 2018

ACKNOWLEDGEMENT

I would like to thank my supervisor, Assoc. Prof. Dr. Yoon Tiem Leong for his guidance and tolerance for my Ph.D. project. I would also like to show my gratitude to Dr. Lim Thong Leng from Multimedia University for his generous help in many topics related to my work. Assoc. Prof. Dr. Chan Huah Yong from the School of Computer Sciences, Universiti Sains Malaysia also provided the computing facility which is imperative in my work. Although we have never met each other, his generous help is highly appreciated.

This research project is not possible without funding. I would like to take this opportunity to express my gratitude to MyPhD scholarship which was offered by the Ministry of Higher Education, Malaysia.

A big thank you to all my labmates who provided me a lively, carefree and joyful working environment. I am too very grateful to my family for their endless support. Lastly, I would like to say both thank you and sorry to my wife. Thank you for being the utmost supportive person to me and sorry for all the time when we are forced to live separately in two different continents.

TABLE OF CONTENTS

Acknowledgement.....	ii
Table of Contents.....	iii
List of Figures.....	vi
List of Abbreviations.....	xiii
Abstrak.....	xiv
Abstract.....	xvii

CHAPTER 1 – INTRODUCTION

1.1 Introduction.....	1
1.2 Motivation of Study.....	1
1.3 Objectives.....	3
1.4 Thesis Overview.....	4

CHAPTER 2 – THEORY AND REVIEW OF CARBON NANOSTRUCTURES

2.1 Brief History of Carbon Allotropes.....	5
2.2 Physics of Fullerene, Carbon Nanotube and Graphene.....	6
2.2.1 Fullerene.....	6
2.2.2 Carbon Nanotube.....	7
2.2.3 Graphene	12
2.3 Hybrid Carbon Nanostructures.....	13
2.4 Review of Carbon Peapods.....	14
2.4.1 Transformation of Peapod into DWCNT.....	16
2.4.2 Applications of Peapods.....	18

2.4.3 Simulations of Carbon Peapods.....	19
2.5 Topology of Carbon Nanostructures.....	21
2.5.1 Euler Characteristic.....	22
2.5.2 Gaussian Curvature.....	26
2.5.3 Gauss-Bonnet Theorem.....	31

**CHAPTER 3 – EFFECTS OF ANNEALING TEMPERATURE ON THE
ANNEALING OF CARBON PEAPOD**

3.1 Introduction.....	33
3.2 Methodology.....	33
3.2.1 Construction of Carbon Peapods.....	33
3.2.2 Molecular Dynamics Simulations.....	37
3.3 Results and Discussions.....	45
3.4 Rings Statistics of Annealed Carbon Peapod Systems.....	56
3.5 Stone-Wales Defects.....	63
3.6 Cross-Linked Defects.....	65
3.7 Concluding Remarks.....	68

**CHAPTER 4 – EFFECTS OF ANNEALING TIME ON THE ANNEALING OF
CARBON PEAPOD**

4.1 Introduction.....	70
4.2 Methodology.....	70
4.3 Results and Discussions.....	72
4.3.1 Defects and Self-Healing Mechanisms (Vacancy Defects).....	77
4.3.2 Defects and Self-Healing Mechanisms (Zipping Mechanism).....	79

4.3.3 Summary of the Self-Healing Process.....	85
4.4 Effects of Total Annealing Time on the Carbon Peapods.....	85
4.4.1 Rings Statistics of Carbon Peapods Annealed for Different Duration.....	89
4.5 Self-Healing of the Diameter of the Annealed Carbon Peapods.....	95
4.6 Concluding Remarks.....	101

CHAPTER 5 – CONCLUSIONS AND FUTURE STUDIES

5.1 Conclusions.....	103
5.2 Future Studies.....	105
5.2.1 Formation of Carbon Foam or Schwarzite through the Annealing of Closely Packed C ₆₀ Molecules.....	105
5.2.2 Ultrahard Cross-linked Derived Hybrid Carbon Nanostructure.....	105

REFERENCES.....	107
------------------------	------------

APPENDIX

LIST OF FIGURES

	Page	
Figure 2.1	Some examples of ball shape fullerenes. (a) C ₂₄ , (b) C ₆₀ , (c) C ₇₀ , (d) C ₇₂ , (e) C ₁₈₀ s and (f) C ₇₂₀ .	7
Figure 2.2	The number of publications with keyword “carbon nanotube” indexed by Web of Science. Note that the data in 2017 is incomplete because this graph is plotted in December 2017.	8
Figure 2.3	Lattice vectors \mathbf{a}_1 and \mathbf{a}_2 shown on a small piece of graphene.	9
Figure 2.4	Some possible choices of n and m shown. In order to create a carbon nanotube of chirality (n, m) , the sheet is rolled from point $(0, 0)$ to the desired chirality. The maximum chiral angle is 30° due to geometrical limitation.	10
Figure 2.5	Cross-section and side view of three SWCNT. (a) Armchair SWCNT(6, 6) where $m = n$. (b) Zigzag SWCNT (10, 0) where m or $n = 0$. (c) Chiral SWCNT (8, 4) where $m \neq n$. Note the moiré pattern in (c) which is not observed in the other two CNT.	11
Figure 2.6	Multi-walled carbon nanotube of four layers. In this case, the individual SWCNT are CNT (6, 6), CNT (16, 6), CNT (25, 6) and CNT (34, 6).	12
Figure 2.7	(a) Top view and (b) side view of a free standing graphene.	13
Figure 2.8	HRTEM images of (a) carbon peapod – fullerenes (C ₆₀) are encapsulated in a SWCNT. (b) Cross-sectional (radial) view of a bunch of carbon peapods.	15
Figure 2.9	HRTEM images and schematics of (a), (b) peapod with zigzag configuration; (c), (d) peapod with chiral configuration; (e), (f) peapod with two-molecule layer configuration.	16

- Figure 2.10 Transmission electron microscopy images of (A) carbon peapod prepared for annealing, (B) carbon peapod being annealed for 14 hours at 800 °C. Few fullerenes pairs are fused shown by the arrows. (C) Carbon peapod being annealed for 14 hours at 1000 °C. Longer fullerenes chains are observed with few C₆₀ molecules still maintain its initial configuration. (D) Carbon peapod being annealed for 14 hours at 1200 °C. Complete transformation from carbon peapod to DWCNT is observed. 17
- Figure 2.11 Sequence of TEM micrograph of coalescence of fullerenes induced with electron irradiation. (A) The initial peapod; (B)–(H) consecutive images taken with an interval of 60–90 seconds during the irradiation. 18
- Figure 2.12 (a) Two halves of C₆₀ placed at both sides of an uncapped CNT (5, 5) (b) A capped CNT (C₁₄₀) is built by joining all three parts in (a) where exactly 12 pentagons are required to build such a closed cage structure. 24
- Figure 2.13 Illustrations of the surfaces with different Gaussian curvatures. (a) A positive Gaussian curvature with both the principal curvatures drawn in red. Both the principal curvatures have the same sign. (b) A negative Gaussian curvature with principal curvatures of opposite sign. (c) A zero Gaussian curvature with one non-zero principal curvature and one zero principle curvature (straight line). (d) A zero Gaussian curvature with no measurable non-zero curvatures. 28
- Figure 2.14 Formation of curved graphene by (a) pentagon ring in the middle can be understood as removing a $\pi/3$ carbon slab and joining the open ends (black lines) together, (b) heptagon ring will require insertion of a $\pi/3$ carbon slab in between the two black lines and (c) octagon ring will require insertion of a $2\pi/3$ carbon slab into the opening. 30
- Figure 3.1 Cross-sections of (a) C₆₀@CNT(13, 5), (b) C₆₀@CNT(14, 7) and (c) C₆₀@CNT(12, 12). The axes pointing towards the reader, top and right are z, y and x respectively. 35
- Figure 3.2 The side view of the carbon peapods used in this study. The total carbon atoms in each carbon peapod system are 2852, 3132 and 3468 for 13C₆₀@CNT(13, 5), 13C₆₀@CNT(14, 7) and 13C₆₀@CNT(12, 12) respectively. A periodic boundary condition is applied along the z-axis. 37

Figure 3.3	The temperature profile used to simulate the annealing process of the carbon peapods. The annealing temperature of 2000 K is a specific example of the annealing temperatures used in this study.	43
Figure 3.4	The shortest path rings in this graph are <i>abcfea</i> , <i>abdfea</i> , <i>bcfdb</i> and <i>dfgd</i> .	44
Figure 3.5	Annealed $13C_{60}@CNT(13, 5)$ peapod systems cooled to room temperature (300 K). The temperatures (T) refer to the annealing temperatures. Note that the peapod system collapsed at 5000 K and the structure was not annealed into a double-walled carbon nanotube.	46
Figure 3.6	Annealed $13C_{60}@CNT(14, 7)$ peapod systems at room temperature (300 K). The temperatures refer to the annealing temperatures.	48
Figure 3.7	Annealed $13C_{60}@CNT(12, 12)$ peapod systems at room temperature (300 K). At $T = 1000$ K, zigzag packing of encapsulated C_{60} is observed inside the outer tube.	50
Figure 3.8	Fullerenes taken from Fig. 3.5 at 2000 K. (i) a-b pair the initial stage of coalescence between two C_{60} . (ii) c-d pair another early stage of coalescence between two C_{60} . Both structures are comparable to the results reported by Han <i>et al.</i> (2004).	52
Figure 3.9	(a) The length/diameter of the annealed inner CNT vs annealing temperature of $13C_{60}@CNT(14, 7)$. (b) The diameter profiles of the inner CNT. The length of the inner CNT is shorter at higher temperature given that the points are more packed as well as a decreased difference between the min/max points.	54
Figure 3.10	Cross-sectional view of $13C_{60}@CNT(12, 12)$ showing an elliptical deformation of the outer CNT.	56
Figure 3.11	Number of Rings vs Annealing temperature of $13C_{60}@CNT(13, 5)$.	59
Figure 3.12	Number of Rings vs Annealing temperature of $13C_{60}@CNT(14, 7)$.	59

Figure 3.13	Number of Rings vs Annealing temperature of $^{13}\text{C}_{60}@CNT(12, 12)$.	60
Figure 3.14	Comparison of number of rings vs annealing temperature between different outer CNT diameters.	62
Figure 3.15	The number of rings of the annealed outer CNT vs annealing temperatures for all three peapod systems. Note that there is no ring count for $^{13}\text{C}_{60}@CNT(13, 5)$ from 4700 K to 5000 K. Octagon rings is not included in this graph as it is zero for all cases.	63
Figure 3.16	Stone-Wales transformation.	63
Figure 3.17	Stone-Wales defects found on the inner CNT of (a) $^{13}\text{C}_{60}@CNT(13, 5)$ annealed at 4500 K (b) $^{13}\text{C}_{60}@CNT(14, 7)$ annealed at 4300 K and (c) $^{13}\text{C}_{60}@CNT(12, 12)$ annealed at 4400 K. All three figures are magnified view of the inner CNT formed after the annealing process.	65
Figure 3.18	Cross-sectional view of $^{13}\text{C}_{60}@CNT(13, 5)$ annealed at 3900 K. A few cross-linked defects are observed where sp^3 bonds are formed between the inner CNT and outer CNT.	67
Figure 3.19	Number of cross-linked defects versus annealing temperature for all three peapod systems. $^{13}\text{C}_{60}@CNT(13, 5)$ is most prone to cross-linked defects due to its tight space for fullerenes resulting in relatively unstable structure compared to two other peapod systems.	67
Figure 4.1	The annealing process of $^{13}\text{C}_{60}@CNT(12, 12)$ at 3500 K. The dashed lines are subroutines in our work that cools down the carbon peapod after every 1 ns of annealing. This graph is not plotted to scale for illustration purpose.	71
Figure 4.2	Pentagons, hexagons, heptagons and octagons vs time. The left Y-axis shows the number of pentagons, heptagons and octagons while the right Y-axis shows the number of hexagons. The molecular structures of a – e are shown in Fig. 4.3.	73

- Figure 4.3 The structures of the carbon peapods at various stages of the annealing process. (a) Carbon peapod before the annealing starts. (b) Carbon peapod being annealed into DWCNT. However the inner CNT is highly corrugated. (c) The structure shows a partially defected inner CNT. (d) The defects are fully healed displaying a good radial separation between the inner CNT and the outer CNT. (e) Final frame of our simulation showing a high quality DWCNT. 76
- Figure 4.4 Number of rings vs annealing time between 14.9 ns to 15.1 ns. The two sharp drops of hexagons are observed at (i) 14.9475 ns and 14.9480 ns (Hexagons drop from 1566 to 1495) and (ii) 14.9565 ns and 14.9570 ns (Hexagons drop from 1505 to 1403). 78
- Figure 4.5 The structures of the defected carbon peapod corresponding to the two instances when sharp drops in hexagons are observed. (a) At 14.948 ns, the outer CNT ruptured with few vacancy defects formed. The defects are coloured in red. (b) At 14.957 ns, more vacancy defects are formed. The inner CNT is also affected near the ruptured outer CNT. The vacancy defects of the outer CNT is colours in red and blue while the defected part of the inner CNT is colours in orange. (c) The rotated (by 90°), magnified and unobstructed view of the defects in (b). The whole defects appear like amorphous carbon network and the inner CNT and outer CNT are found to be bonded in a messy fashion. 79
- Figure 4.6 Various stages of self-healing mechanism of the defected DWCNT. The DWCNT are shown in pair where the second DWCNT is a 90° rotation of the first DWCNT. The zipping mechanism that zips up the graphene slab always occurs at the interstitial site between the inner CNT and graphene slab. The sp³ bonds between the graphene slab and the outer CNT holds the inner CNT in position and remained until the last stages of zipping. The sp³ bonds are eventually broken and the inner CNT is detached completely from the outer CNT. 82

- Figure 4.7 Sequence of atom rearrangements that results in a net gain of positive Gaussian curvature. (a) The overall structural view of the DWCNT at time = 32.8395 ns. The few highlighted atoms are located at the interstitial site between the inner CNT and graphene slab. (b) The magnified view of the 10 highlighted carbon atoms shown in (a). The yellow arrow indicates the direction of the rest of the inner CNT which is not affected by the vacancy defect. The L-shape blue boxes is where the graphene slab is bonded (sp^3) to the outer CNT. In between the blue boxes and the highlighted carbon atoms is the hollow end of that inner CNT. (c) Atom 1 bonded with atom 5 which breaks its bond with atom 4. A decagon ring is formed. (d) Atom 5 is bonded with atom 4 again forming a pentagon/heptagon pair. (e) Atom 6 bonded with atom 4 which break its bond with atom 5 to form a more stable hexagon/hexagon pair. A net gain of $\pi/3$ Gaussian curvature on the surface of the 10 atoms. However, it should be noted that Kroes *et al.* (2015) argued that AIREBO might not produce the shortest pathway for the rearrangement process. It is important to know the limitations of the classical potential when it comes to the simulations of vacancy defects. In fact the whole repair process will probably be different if first principles molecular dynamics is used. However this is impossible (computation wise) due to the size of the studied system. 84
- Figure 4.8 The annealed carbon peapods with different total annealing time. The temperature is 300 K since they are cooled to room temperature. 86
- Figure 4.9 Number of rings vs annealing time. The left Y-axis shows the number of pentagons, heptagons and octagons while the right Y-axis shows the number of hexagons. 90
- Figure 4.10 $R_5 - R_7$ and $R_5 - R_7 - 2R_8$ vs annealing time. Note that both calculated rings differences converge at 12. 91
- Figure 4.11 The calculated rings differences show that the topology of our inner CNT to be consistent with the topology of a capped SWCNT. 93
- Figure 4.12 The calculated rings differences show that the topology of our outer CNT to be consistent with the topology of a torus. 93

- Figure 4.13 (a) The octagon ring found on the outer CNT after the carbon peapod is being annealed for 76 ns. (b) No octagon ring found on the outer CNT after the carbon peapod is being annealed for 77 ns. Notice that the side view of (b) 77 ns is flatter than (a) because octagon ring creates a sharper local curvature (a dent in this case). (c) and (d) show the magnified rings structures in (a) and (b) respectively. With an additional annealing time of 1 ns, R_8 and R_6^{one} are transformed into two heptagons rings (R_7^{one} and R_7^{two}). Note that R_6^{two} and R_5^{one} switched their configuration to R_5^{two} and R_6^{three} as a consequence of the geometry changes. 94
- Figure 4.14 The calculated average diameter of the outer CNT is plotted against the annealing time. The average diameter is very close to the diameter of a perfect CNT(12, 12) of 16.27 Å. 96
- Figure 4.15 (i) Outer CNT annealed for 40 ns. (ii) Outer CNT annealed for 100 ns. (iii) to (vi) are the diameter profiles of the outer CNT annealed for different total time. Point **a** to **h** are the corresponding visualizations of the bumps/dents and their corresponding diameters. Bumps **d** and **h** are more curved than they appear in 4.15(ii) but we are limited to a 2D visualization of the structure. 97
- Figure 4.16 (i) Minimum diameter of the outer CNT vs annealing time with a 14.2 Å line which is the diameter of outer CNT that allows an ideal van der Waals separation. Increased annealing time increases the diameter to roughly 14.2 Å which allows the inner CNT to pass through the bottleneck. (ii) to (v) Minimum diameter profiles of outer CNT annealed at 40 ns, 60 ns, 80 ns and 100 ns. The minimum points of the diameter profiles are plotted in Fig. 4.16(i). 100
- Figure 4.17 Inner CNT length of the annealed peapod at room temperature vs their respective total annealing time. The reduced length of the inner CNT plateaued after 65 ns which coincides with the time when $R_5 - R_7 - 2R_8 = 12$. 101

LIST OF ABBREVIATIONS

CNT	Carbon Nanotube(s). It can either be singular or plural.
DWCNT	Double-walled Carbon Nanotube(s). It can either be singular or plural.
EC	Euler Characteristic
LAMMPS	Large-scale Atomic/Molecular Massively Parallel Simulator
MD	Molecular Dynamics
MWCNT	Multi-walled Carbon Nanotube(s). It can either be singular or plural.
S-W	Stone-Wales
SWCNT	Single-walled Carbon Nanotube(s). It can either be singular or plural.

PENGAJIAN DINAMIK MOLEKUL BAGI PENYEPUHLINDAPAN

PEAPOD KARBON

ABSTRAK

Dalam tempoh 30 tahun yang lalu, karbon terus mengejutkan masyarakat saintifik memandangkan andaian sebelum ini bahawa semua struktur karbon sudah diketahui. Salain daripada grafit, intan dan amorfus; alotrop karbon baru termasuk fullerene, nanotub karbon (CNT) dan graphene telah ditemui pada tahun 1985, 1991 dan 2004. Peapod karbon adalah nanostruktur karbon kacukan di mana fullerene seperti C_{60} dikurungkan dalam nanotub karbon luar. Peapod karbon boleh diubah menjadi nanotub karbon dwi-dinding (DWCNT) melalui proses penyepuhllindapan. Pada dasarnya, fullerene akan bercantum dan menjadi CNT yang lebih kecil di dalam CNT luaran yang bertindak sebagai acuan/kontena. Walau bagaimanapun terdapat beberapa jurang penyelidikan dalam simulasi proses penyepuhllindapan; contohnya, potensi tidak digunakan untuk CNT luar peapod dan interaksi jarak jauh (van der Waals) juga diabaikan. Dalam tesis ini, tiga peapod karbon dengan diameter yang berbeza direka bentuk berdasarkan keputusan eksperimen. Tiga peapod karbon tersebut adalah $13C_{60}@CNT(13, 5)$, $13C_{60}@CNT(14, 7)$ dan $13C_{60}@CNT(12, 12)$ di mana terdapat 13 molekul C_{60} dalam setiap peapod karbon. Simulasi dinamik molekul (MD) klasik dijalankan untuk mengkaji perubahan peapod karbon ke DWCNT bagi seluruh proses penyepuhllindapan untuk tempoh 1 ns. Semua simulasi MD dilakukan dengan LAMMPS dan AIREBO dipilih sebagai potensi untuk mensimulasikan interaksi antara molekul dan dalam molekul antara atom-atom karbon. Keputusan simulasi menunjukkan bahawa reaktiviti peapod karbon meningkat dengan peningkatan suhu penyepuhllindapan. Peapod karbon didapati berubah ke DWCNT

pada suhu penyepuhlindapan melebihi 3500 K. Cincin-cincin karbon yang didapati dalam bentuk pentagon, heksagon, heptagon dan oktagon juga diukur secara numerik dan dikira dari struktur-struktur yang telah disepuhlindapkan. Statistik cincin menunjukkan hubungan rapat antara struktur dan bilangan cincin. Terutamanya apabila bilangan pentagon dan heptagon adalah hampir sama, strukturnya adalah dalam bentuk DWCNT yang disepuhlindap sepenuhnya. Kecacatan lapisan tersilang dalam peapod karbon yang disepuhlindapkan juga dikaji. Didapati bahawa $13C_{60}@CNT(13, 5)$ mempunyai kecacatan lapisan tersilang yang terbanyak disebabkan konfigurasi ketat. Bahagian kedua tesis ini melibatkan $13C_{60}@CNT(12, 12)$ yang disepuhlindap untuk 100 ns pada 3500 K. Jumlah masa penyepuhlindapan adalah 100 kali lebih lama daripada seksyen sebelum ini. Pada masa 15 ns, struktur didapati runtuh pada satu hujung CNT dalaman bersama dengan CNT luaran yang berdekatan. Selepas itu, yang menakjubkan, struktur itu berjaya menyembuhkan diri sendiri semasa proses penyepuhlindapan. Siasatan lanjutan mendedahkan mekanisme penyembuhan diri itu berlaku dalam dua peringkat. Peringkat pertama penyembuhan diri adalah melalui pembinaan kembali kekosongan dan peringkat kedua adalah mekanisme zipping. Kualiti DWCNT yang disepuhlindap just dibandingkan dengan masa penyepuhlindapan yang berbeza. Melalui pelaksanaan subrutin pada simulasi utama, 100 struktur DWCNT yang telah disepuhlindapkan selama 1 ns, 2 ns, 3 ns ... 99 ns dan 100 ns telah diperolehi. Perbezaan tetap pada 12 antara bilangan pentagon dan heptagon diperhatikan untuk struktur yang disepuhlindap lebih daripada 77 ns. Pemerhatian ini adalah berkaitan dengan ciri-ciri Euler sistem karbon. Penyiasatan lanjutan mendedahkan bahawa topologi peapod karbon yang disepuhlindapkan dalam simulasi ini adalah sepadan dengan topologi DWCNT yang sempurna. Akhir sekali, ia

patut ditekankan bahawa keputusan simulasi baharu yang dibentangkan dalam tesis ini tidak mungkin didedahkan tanpa masa simulasi yang tersangat panjang.

MOLECULAR DYNAMICS STUDIES OF THE ANNEALING OF CARBON PEAPODS

ABSTRACT

In the past 30 years, carbon kept surprising the scientific community given the previous assumption that all carbon structures are already known. Apart from graphite, diamond and amorphous; new carbon allotropes including fullerenes, carbon nanotubes (CNT) and graphenes were discovered in year 1985, 1991 and 2004 respectively. Carbon peapod is a hybrid carbon nanostructure in which fullerenes such as C_{60} are encapsulated in an outer carbon nanotube. Carbon peapod can be transformed into a double-walled carbon nanotube (DWCNT) through annealing process. In essence, the fullerenes will fuse and form a smaller CNT in the outer CNT which acts as a mold/container. However there are a few research gaps in the simulations of the annealing process, e.g., potential was not applied to the outer CNT of the peapod and long range (van der Waals) interactions was ignored. In this thesis, the structures of three carbon peapods with different diameters are first constructed based on experimentally measured data. The peapods in the study are $13C_{60}@CNT(13, 5)$, $13C_{60}@CNT(14, 7)$ and $13C_{60}@CNT(12, 12)$, where there are 13 C_{60} molecules in each peapod. Classical molecular dynamics (MD) simulations are performed to study the morphological transition of carbon peapods into DWCNT for the whole annealing process which lasted for 1 ns. All MD simulations are done with LAMMPS and AIREBO is chosen as the potential to simulate the inter- and intra-molecular interactions among the carbon atoms. From the simulated results it is observed that increased reactivity of the carbon peapod is associated with increasing annealing temperature. The carbon peapods transformed into DWCNT at an annealing

temperature higher than 3500 K. The number of carbon rings, i.e., pentagon, hexagon, heptagon and octagon of the carbon peapods are numerically measured and sampled from the annealed structures. The rings statistics reveal an intimate relationship between the structures and the rings counts. In particular, it is found that when pentagons and heptagons are roughly the same in number, the structure is a fully annealed DWCNT. The cross-linked defects of the annealed peapods are also studied. It is found that $^{13}\text{C}_{60}@\text{CNT}(13, 5)$ has the highest cross-linked defects across all annealing temperatures due to its tight configuration. In the second part of the study, $^{13}\text{C}_{60}@\text{CNT}(12, 12)$ is annealed for 100 ns at 3500 K. The simulation period is 100 times longer than that of the previous section. While still being annealed at 15 ns, it is discovered that the structure collapses at one end of the inner CNT together with its nearby outer CNT. Surprisingly after that, the structure manages to salvage itself during the annealing process. Further investigation reveals that the self-healing mechanism occurs in two stages. The first stage of the self-healing is through vacancy reconstruction and the second stage is via the zipping mechanism. The quality of the annealed DWCNT with different annealing time are also compared. Through the execution of subroutines on the main simulations, 100 DWCNT which have been annealed for 1 ns, 2 ns, 3 ns ... 99 ns and 100 ns are obtained. It is observed that the numbers of pentagons and heptagons in the structures annealed for more than 77 ns differ constantly by a margin of 12. The observation is interpreted in terms of the Euler characteristic of the carbon systems being simulated. Further investigation reveals that the topology of the annealed carbon peapod matches the topology of a pristine DWCNT. Finally, it should be emphasized that the novel simulated results presented in this thesis would not be possibly revealed if not for the lengthy simulation time.

CHAPTER 1 INTRODUCTION

1.1 Introduction

Carbon peapod is a hybrid nanostructure where fullerenes such as C_{60} or C_{70} are inserted into carbon nanotube (CNT). Carbon peapod has been known to transform into double-walled carbon nanotube (DWCNT) through annealing process. While carbon peapods have been studied extensively both experimentally and theoretically, there are still phenomena not fully understood in the process of the annealing process.

1.2 Motivation of Study

The transformation process of the carbon peapods into DWCNT can be studied using molecular dynamics (MD) simulations. Previous MD simulations (Hernández *et al.*, 2003; Shibuta and Maruyama, 2006; Suarez-Martinez *et al.*, 2010) have shown interesting atomistic details particularly the coalescences process that connect two or more fullerenes into a single larger fullerene. However in those simulations, the outer CNT is treated as a non-interacting layer acting only as a container to those fullerenes in it. In other words, the effects of the long-range interactions between the outer CNT and the inner fullerenes as well as the short-range interactions within the outer CNT are not considered in the said annealing simulations. Justifications are given for the exclusion of the interactions mentioned above. First, the outer CNT is much more stable than the fullerenes thus having no role in the coalescences process. Secondly, the system will be much larger due to the additional atoms and interactions and this requires a much higher computation power. Yet the given justifications can become a blind spot when it comes to simulations. The annealing temperatures used in molecular dynamics simulations are very high ranging from 2000 K to 4000 K; it is unlikely that

the carbon atoms are as stable as their counterparts in experiments (roughly 1500 K). In experiment (Krasheninnikov and Banhart, 2007), carbon peapod to DWCNT transformations induced by irradiation are observed to have high contact point temperature of at least 2000 K. The outer CNT is found to fuse with the inner CNT forming cross-linked defects. This is another evidence where the outer CNT can affect the coalescences process.

Furthermore the MD simulations mentioned above usually have simulation durations in the range of few nanoseconds. The simulation duration is taken as such presumably because the peapod structures is observed to be transformed into DWCNT. This raises the question about the required simulation duration for a complete transformation. “Completion” of the transformation of the carbon peapod into DWCNT remained ill defined. This is where the suitability of the analytical methods of the simulations results comes in. In previous works, the completion of the annealing process is decided by examining the molecular structures through visual inspections. While the observation of two CNT does indicates a DWCNT structure, there exists a significant gap between a corrugated and irregular inner CNT and a uniform high quality inner CNT. There should be a way to quantify or identify the transitional time step where the resulting DWCNT is of high quality.

1.3 Objectives

Based on the research gaps discussed in section 1.2, there are three primary objectives and methods for: (1) Inter-molecular interactions between outer CNT and inner CNT/fullerenes and intra-molecular interactions within the outer CNT, (2) increment of the simulation duration, and (3) other ways to analyze the simulations results.

For (1), short-range and long-range potentials must be applied to all atoms in the designed carbon peapod structure. A suitable potential or combinations of potentials must be identified in order to have accurate simulations within reasonable timeframe. Potentials are chosen based on their physics, modelling suitability and computation efficiency. Once the potential is chosen, the simulation system itself must be designed such that it can mimic or reproduce previous works by others. There are many parameters which need to be decided before one can run a reasonably accurate simulation. The parameters including but not limited to the total number of atoms, diameter of the CNT, simulation box size, types of boundary conditions, approach for simulated annealing, parameterizations of the potential and thermostats. This is followed by (2) where the simulation duration is extended. One can choose to do multiple extension where the structure is annealed for different durations. Based on the simulation setup, one should also roughly estimate the computation time needed for the extended simulations to avoid unnecessary waiting. Unfortunately for (3), there is no straightforward way to come out with a different analytical method. However, one can always start by re-examining the methods used to analyse results in relevant simulations work. In the MD simulations of carbon peapods, some of the studied physical properties include the diameter of the carbon peapod, the sp^2/sp^3 bonds ratio, carbon rings statistics, energetics and others. The topological and geometrical

properties of the molecular structures should also be considered apart from the physical properties mentioned above.

1.4 Thesis Overview

In Chapter 2, the physics of carbon nanostructures such as fullerenes, CNT, graphene and carbon peapods are reviewed. The geometrical and topological descriptions of carbon nanostructures, particularly the Euler characteristic and Gaussian curvature are also introduced. In Chapter 3, the effects of annealing temperature on the transformation process from carbon peapod to DWCNT are studied. Results are presented in illustrations of the actual structures, analysis of the rings counts and the number of cross-linked defects. In Chapter 4, the effects of annealing time on the carbon peapod are explored. First part of the results focuses on the self-healing mechanism where the defected DWCNT is healed into a DWCNT. The second part focuses on the geometrical and topological analysis of the annealed structure at different total annealing time. The last part in Chapter 4 studies the diameters changes of the outer CNT and inner CNT. Chapter 5 discusses some possible future studies based on the molecular dynamics simulations of carbon systems. Appendix on the computations of the CNT diameters is also included.

CHAPTER 2 THEORY AND REVIEW OF CARBON NANOSTRUCTURES

2.1 Brief History of Carbon Allotropes

Carbon has been known since human civilizations in the forms of charcoal. In 18th century, advancements in the understanding of carbon is seen where visually different materials like charcoal and diamond are known to be made of the same element by Antoine Lavoisier.

For more than 200 years, it has been thought that carbon allotropes are just graphite, diamond and amorphous. In 1985, a surprise discovery made by Kroto *et al.* where a new carbon allotrope specifically C₆₀ was synthesized by laser irradiation on graphite. The new carbon allotrope is now known as fullerene and C₆₀ is a member of the allotrope. Harold Kroto also named C₆₀ Buckminsterfullerene because geodesic domes (designed by Buckminster Fuller) is similar to the truncated icosahedron structure of C₆₀.

In 1991, six years after the discovery of fullerene, Sumio Iijima published his most cited work on the discovery of multi-walled carbon nanotube (Iijima, 1991). The discovery of carbon nanotube and the scientists responsible for the work have been a subject of dispute. According to Monthieux and Kuznetsov (2006), carbon nanotube was in fact discovered back in 1952 by L. V. Radushkevich and V. M. Lukyanovich. However it is no dispute that Sumio Iijima is the one who popularized and ignited the interest of research in carbon nanotubes. In 1993, Iijima and Ichihashi successfully synthesized single-walled carbon nanotube which was one of the smallest one-dimensional systems observed at the time.

In 2004, Andre Geim and Konstantin Novoselov surprised the world by showing a monolayer 2D carbon structure known as graphene. They are able to prepare

graphene by mechanical exfoliation with adhesive tape through repeated peeling process. Since then, other two-dimensional atomic crystals based on graphene are found, *e.g.*, hexagonal boron nitride (hBN), molybdenum disulphide (MoS₂) and fluorographene.

2.2 Physics of Fullerene, Carbon Nanotube and Graphene

Carbon nanostructures are grouped based on their dimension. Fullerenes being the 0D materials, carbon nanotubes being the 1D materials and graphene being the 2D materials.

2.2.1 Fullerene

Fullerenes or more specifically C₆₀ which was synthesized by Kroto *et al.* in year 1985. C₆₀ is shaped like a truncated icosahedron, essentially the shape of a football. Since the discovery of C₆₀ in 1985, scientists have managed to figure out many more members belonging to the family of fullerenes. Some of the examples include C₂₀, C₂₄, C₆₀, C₇₀, C₇₂, C₈₀, C₁₈₀, C₇₂₀ and many more. While many fullerenes are synthesized in experiment, some fullerenes especially the very small ones, *e.g.*, C₂₀ and C₂₄ are only found indirectly as functionalized fullerenes (Wang *et al.*, 2001). Once thought to be man-made material, C₆₀ and C₇₀ are also found naturally in rock from Russia (Buseck *et al.*, 1992). Besides that, there are also fullerenes with heptagon and/or octagon rings that further complicate the geometry of the fullerenes (Tan *et al.*, 2011). Later in this chapter, the mathematical modeling of the fullerenes based on its ring members using Euler characteristic will be discussed. In Fig. 2.1, a few members of the fullerenes family including the well-known C₆₀ and C₇₀ are shown.

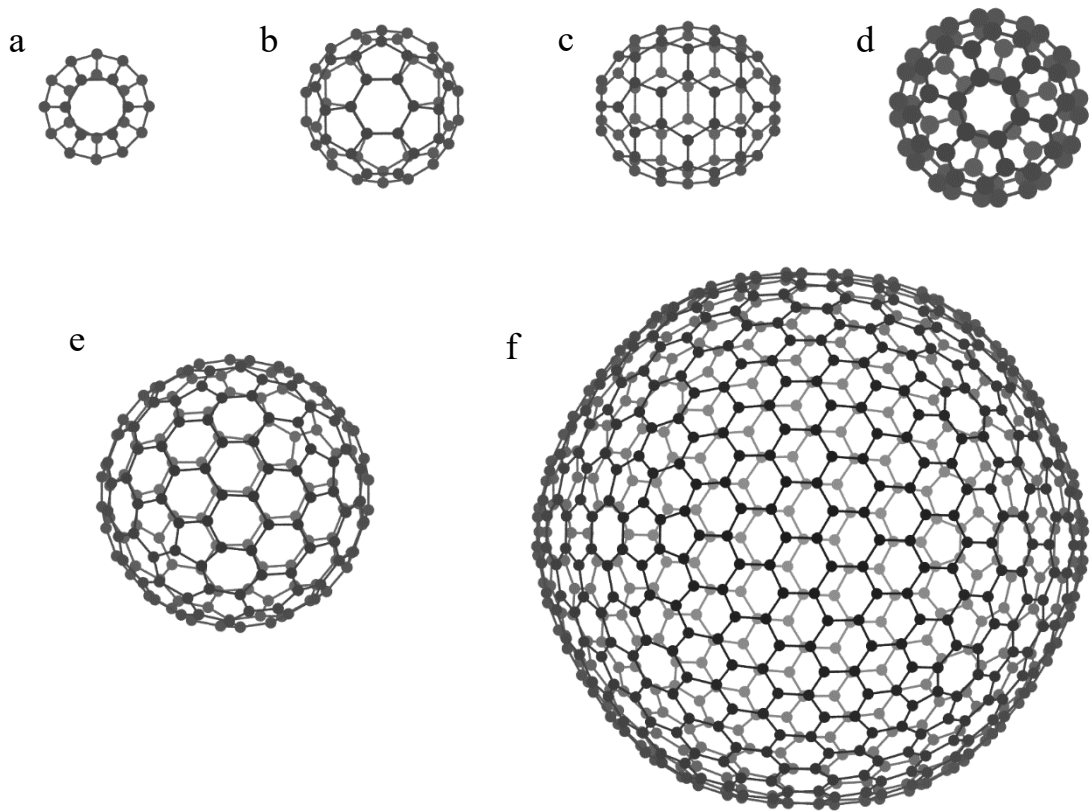


Figure 2.1: Some examples of ball shape fullerenes. (a) C_{24} , (b) C_{60} , (c) C_{70} , (d) C_{72} , (e) C_{180} and (f) C_{720} .

2.2.2 Carbon Nanotube

Since the work by Iijima (1991), an ever increasing research interest in CNT is observed even after almost 28 years. Here the number of publications with the keyword “carbon nanotube” versus the year of publication is plotted in Fig. 2.2. Note that the quotation marks are meant to restrict the search to “carbon nanotube” only. The keywords “carbon” and “nanotube” as individual search term will be searched if quotation marks are not used.

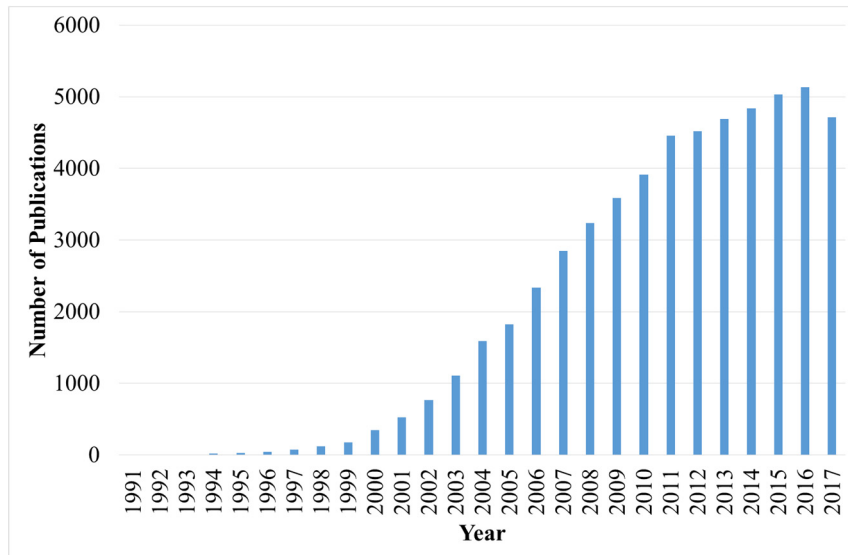


Figure 2.2: The number of publications with keyword “carbon nanotube” indexed by Web of Science. Note that the data in 2017 is incomplete because this graph is plotted in December 2017.

Carbon nanotube is a collective term for different groups of carbon nanostructures sharing similarity of its tubular appearance. First there are the single-walled carbon nanotubes (SWCNT) and multi-walled carbon nanotubes (MWCNT). MWCNT can be imagined as a SWCNT inserted into another SWCNT with larger diameter and the process is repeated with the most outer SWCNT having the largest diameter. For SWCNT, there are three types of CNT, i.e., armchair, zigzag and chiral. The construction of each type of CNT is dependent on the chiral angle one choose to roll the graphene which is the basic building block for CNT. SWCNT can be either metallic or semiconducting with its bandgap ranging from 0.5 eV to 2.0 eV (Wilder *et al.*, 1998). The basic building block, the lattice vectors \mathbf{a}_1 and \mathbf{a}_2 is shown in Fig. 2.3.

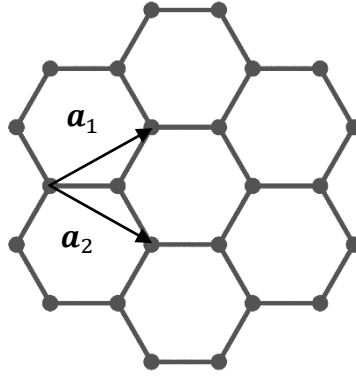


Figure 2.3: Lattice vectors \mathbf{a}_1 and \mathbf{a}_2 shown on a small piece of graphene.

Lattice vectors \mathbf{a}_1 and \mathbf{a}_2 are defined as follows,

$$\mathbf{a}_1 = \left(\frac{3}{2} a_{cc}, \frac{\sqrt{3}}{2} a_{cc} \right), \mathbf{a}_2 = \left(\frac{3}{2} a_{cc}, -\frac{\sqrt{3}}{2} a_{cc} \right) \quad 2.1$$

where a_{cc} is the carbon-carbon bond length ($a_{cc} = 1.42 \text{ \AA}$). So the magnitudes of the lattice vectors are simply,

$$a = |\mathbf{a}_1| = |\mathbf{a}_2| = \sqrt{3} \times 1.42 \text{ \AA} = 2.46 \text{ \AA}. \quad 2.2$$

The chiral vector or perimeter vector, \mathbf{c} is

$$\mathbf{c} = n\mathbf{a}_1 + m\mathbf{a}_2 \quad 2.3$$

where n and m are the chirality parameters. Fig. 2.4 shows some of the possible choices of n and m (Saito *et al.*, 1992) on a graphene sheet.

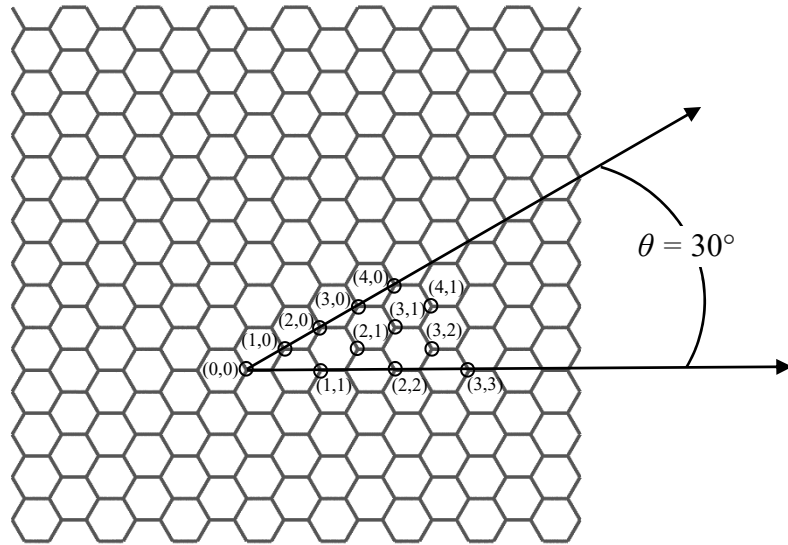


Figure 2.4: Some possible choices of n and m shown. In order to create a carbon nanotube of chirality (n, m) , the sheet is rolled from point $(0, 0)$ to the desired chirality. The maximum chiral angle is 30° due to geometrical limitation.

The chiral angle for a zigzag CNT is 0° and the chiral angle for an armchair CNT is 30° . The chiral angle (between 0° to 30°) depends on the chirality parameters n and m that one chooses. In Fig. 2.5, examples of all three types of SWCNT are shown. The diameter of CNT, d can also be calculated with the magnitude of the chiral vector,

$$\pi d = \|c\| \quad 2.4$$

$$d = \frac{2.46 \text{ \AA}}{\pi} \sqrt{(n^2 + m^2 + nm)}. \quad 2.5$$

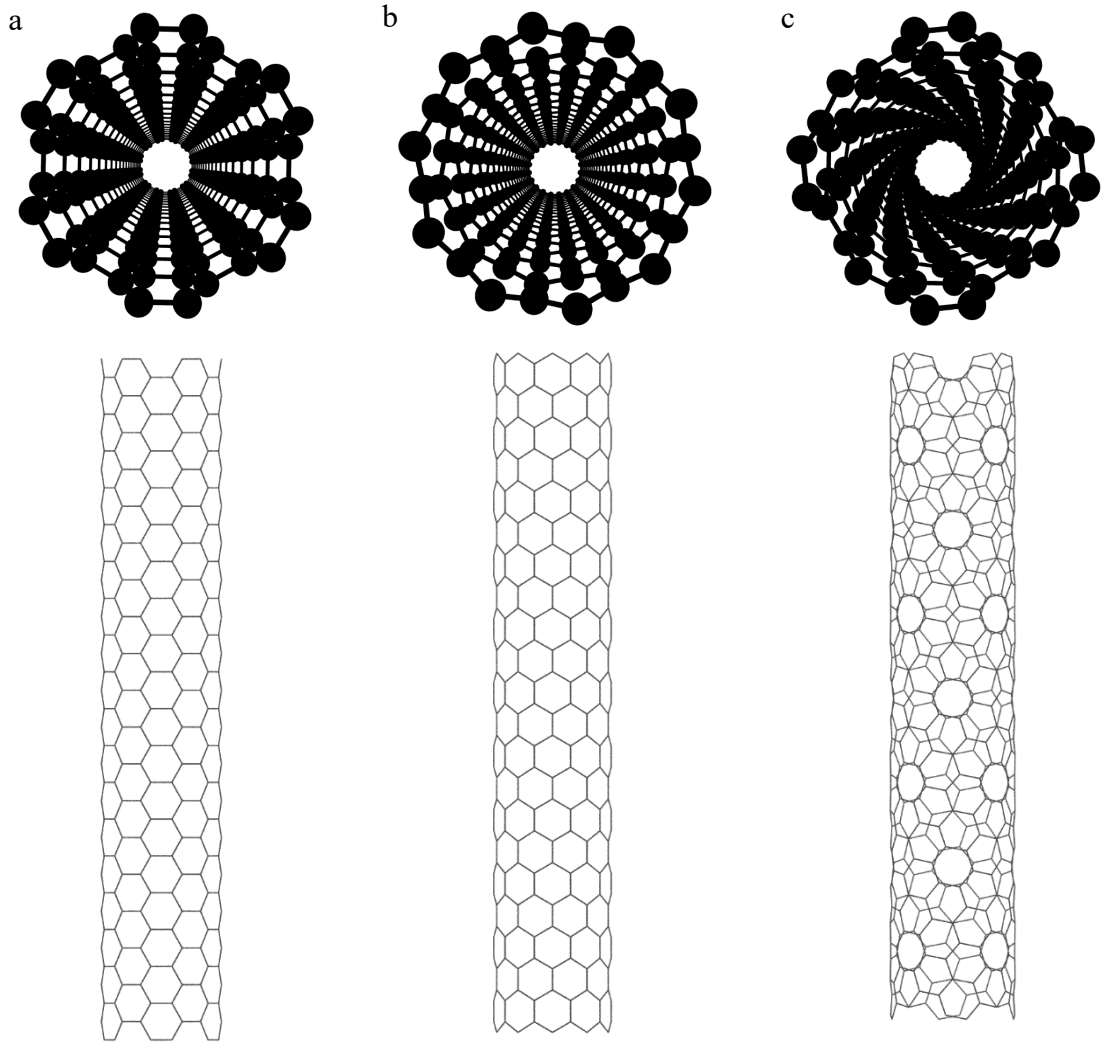


Figure 2.5: Cross-section and side view of three SWCNT. (a) Armchair SWCNT(6, 6) where $m = n$. (b) Zigzag SWCNT (10, 0) where m or $n = 0$. (c) Chiral SWCNT (8, 4) where $m \neq n$. Note the moiré pattern in (c) which is not observed in the other two CNT.

Multi-walled carbon nanotube (MWCNT) is made of at least two individual SWCNT with different diameters. Double-walled carbon nanotube (DWCNT) is also part of the MWCNT family but is usually referred by its own name (DWCNT). The SWCNT with larger diameter encloses the SWCNT with smaller diameter and the minimum van der Waals separation between two SWCNT is roughly 3.4 Å. An example of MWCNT is shown in Fig. 2.6.

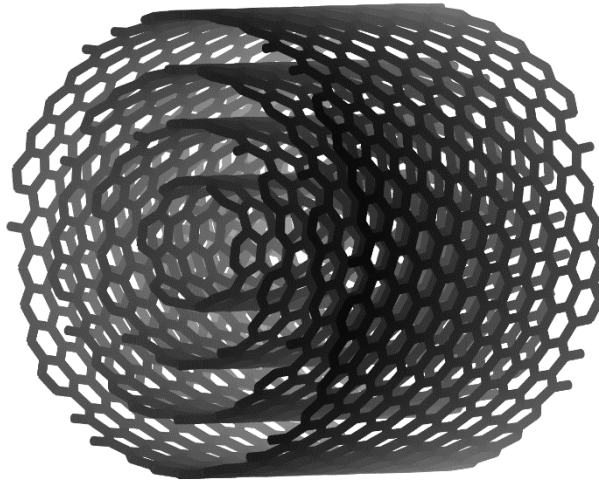


Figure 2.6: Multi-walled carbon nanotube of four layers. In this case, the individual SWCNT are CNT (6, 6), CNT (16, 6), CNT (25, 6) and CNT (34, 6).

2.2.3 Graphene

Landau (1937) and Landau and Lifshitz (1980) argued that freestanding 2D materials such as graphene cannot exist because they are thermodynamically unstable. At finite temperature, the thermal fluctuations in low-dimensional crystal lattices will lead to atomic dislocation so big that it is comparable to the interatomic distances. However this was proven wrong when Novoselov *et al.* (2004) were able to extract a single layer, freestanding graphene through mechanical exfoliation.

Graphene is a single layer of carbon atoms arranged in hexagonal lattice. This makes it the first material to have a thickness of just one atom, thus the classification of graphene as the first known 2D material. Fig. 2.7 shows a piece of graphene with the top view (essentially the same as Fig. 2.4) and the side view of it. When stacked together, many layers of graphene will form graphitic structure which has an interlayer van der Waals distance of 3.35 Å. In fact, the first graphene was extracted from graphite (Novoselov *et al.*, 2004).

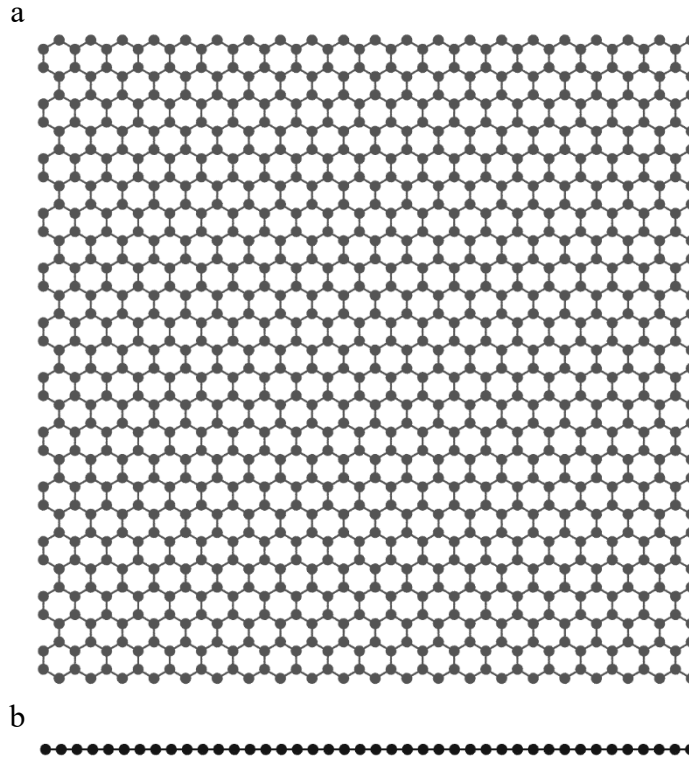


Figure 2.7: (a) Top view and (b) side view of a free standing graphene.

Graphene was found to possess incredible properties. Mechanically, graphene is the strongest material ever measured with a breaking strength of 42 Nm^{-1} and Young's modulus of 1 TPa (Lee *et al.*, 2008). On the electronic properties, graphene is also found to possess 2D gas of massless Dirac fermions (Novoselov *et al.*, 2005) as well as ultrahigh electron mobility of $200,000 \text{ cm}^2\text{V}^{-1}\text{s}^{-1}$ (Bolotin *et al.*, 2007). Thermodynamics of graphene also showed that the thermal conductivity is above $5000 \text{ Wm}^{-1}\text{K}^{-1}$ (Balandin *et al.*, 2008).

2.3 Hybrid Carbon Nanostructures

Perhaps one of the most interesting things that can be done with carbon nanostructures is their flexibility to act as a building block to create new hybrid

nanostructures. It can be either with their carbon counterparts or non-carbon based nanostructures. One example of those is van der Waals heterostructure (Geim and Grigorieva, 2013) in which the basic building blocks are 2D materials such as graphene, hBN, MoS₂, WSe₂ and fluorographene. The combinations of different 2D materials of different total layers will result in unique electronic, optical and mechanical properties. It is a type of nano-engineering made possible with the different basic building blocks.

Another hybrid nanostructure is the carbon peapod. The basic building blocks are CNT and fullerenes with the CNT acting as the shell containing the fullerenes. Due to the many types of CNT and fullerenes known to scientists, carbon peapods can provide rich physics with all the possible variants.

2.4 Review of Carbon Peapods

Since the popularization of research in CNT by Iijima (1991), carbon peapod is speculated to exist because C₆₀ van der Waals distance of 7.1 Å, theoretically can be fitted into a SWCNT with diameter larger than 14.2 Å. Carbon peapod was first discovered by Smith *et al.* (1998) using high-resolution transmission electron microscope (HRTEM) which is shown in Fig. 2.8. Two further publications by the same group (Smith *et al.*, 1999; Smith and Luzzi, 2000) showed the observation of the coalescences of the fullerenes; but the idea of treating it as a method of producing DWCNT was not clear back then.

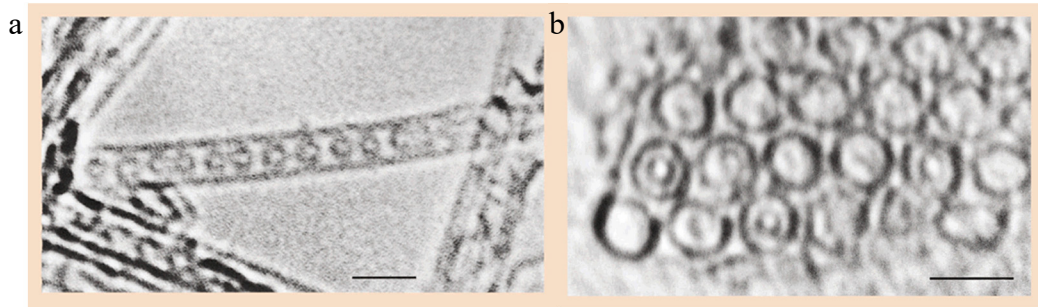


Figure 2.8: HRTEM images of (a) carbon peapod – fullerenes (C_{60}) are encapsulated in a SWCNT. (b) Cross-sectional (radial) view of a bunch of carbon peapods.

Reprinted by permission from Springer Customer Service Centre GmbH: Nature, Smith *et al.*, “Encapsulated C_{60} in carbon nanotubes”, *Nature* 396, 323–324, Copyright (1998).

Since carbon peapods are made of fullerenes and CNT, the variations of carbon peapods are heightened with the variations of the components themselves. Fullerenes can be paired with SWCNT (Smith *et al.*, 1998) or MWCNT (Khlobystov, 2004) to make carbon peapods. The fullerenes can also be C_{60} , C_{70} , C_{72} or other sizes. They can also be functionalized fullerenes (Britz *et al.*, 2004), endohedral fullerenes which are fullerenes acting as cages to contain atoms, ions or clusters (Hirahara *et al.*, 2000) as well as fullerenes with different carbon isotope, *e.g.*, ^{13}C (Simon *et al.*, 2005). The way fullerenes arranged in the CNT also is also different. Depending on the diameter of the outer CNT and the density of the fullerenes, the fullerenes (Fig. 2.90) can be packed differently (Khlobystov *et al.*, 2004). In this work, only the zigzag packing is observed since the diameter of the outer CNT is not large enough to form the other two types of packing. There is also another peapod variant where the diameter of the outer CNT is too large and collapses on itself (Barzegar *et al.*, 2015). The fullerenes are found to be arranged at both sides of the CNT forming a dumbbell shape if viewed at the cross-section.

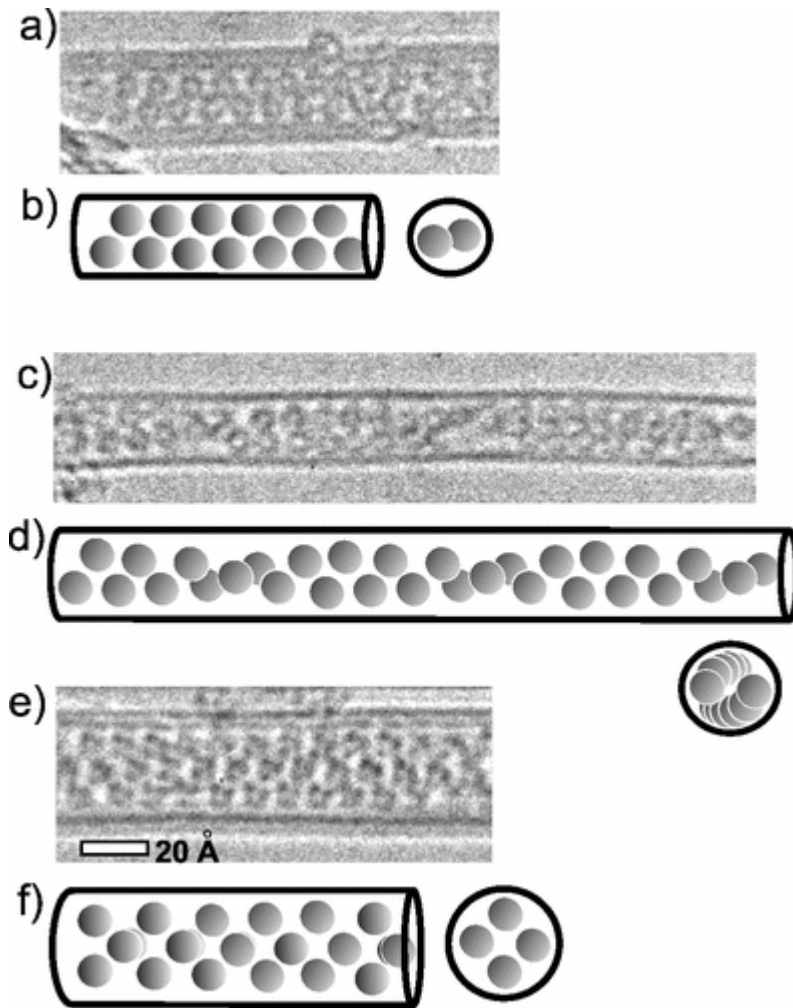


Figure 2.9: HRTEM images and schematics of (a), (b) peapod with zigzag configuration; (c), (d) peapod with chiral configuration; (e), (f) peapod with two-molecule layer configuration.

Reprinted FIG. 2 with permission from Khlobystov *et al.*, “Observation of ordered phases of fullerenes in carbon nanotubes”, *Phys. Rev. Lett.* 92, 245507 (2004). Copyright (2004) by the American Physical Society.

2.4.1 Transformation of Peapod into DWCNT

Using Raman spectroscopy and annealing of the peapod at 1200 °C, Bandow *et al.* (2001) showed that it is possible to produce high quality DWCNT from carbon peapod (Fig. 2.10). They measured the resulting DWCNT and found that the diameter of the inner CNT is determined by the diameter of the outer CNT. Another way to induce the transformation is through electron irradiation (Hernández *et al.*, 2003).

They have found some damage on the SWCNT particularly visible in G and H (Fig. 2.11).

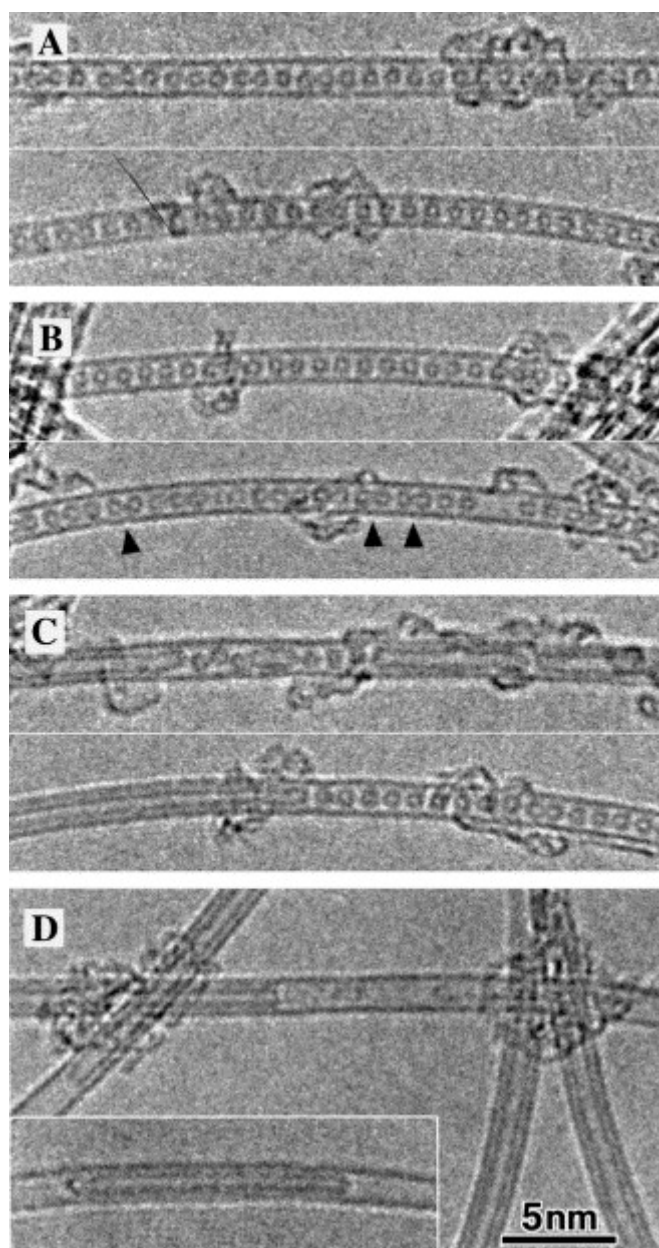


Figure 2.10: Transmission electron microscopy images of (A) carbon peapod prepared for annealing, (B) carbon peapod being annealed for 14 hours at 800 °C. Few fullerenes pairs are fused shown by the arrows. (C) Carbon peapod being annealed for 14 hours at 1000 °C. Longer fullerenes chains are observed with few C₆₀ molecules still maintain its initial configuration. (D) Carbon peapod being annealed for 14 hours at 1200 °C. Complete transformation from carbon peapod to DWCNT is observed.

Reprinted from *Chem. Phys. Lett.* 337, Bandow *et al.*, “Raman scattering study of double-wall carbon nanotubes derived from the chains of fullerenes in single-wall carbon nanotubes”, 48 – 54, Copyright (2001), with permission from Elsevier.

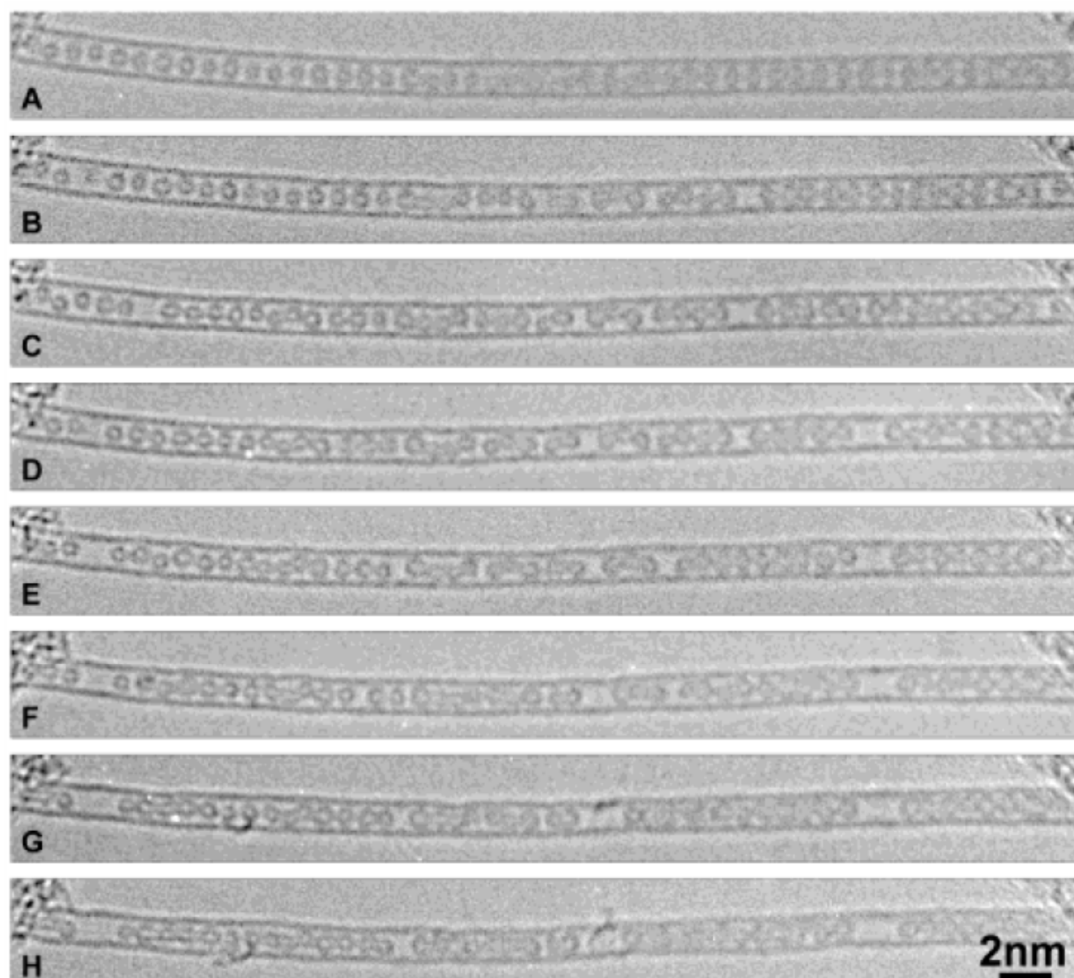


Figure 2.11: Sequence of TEM micrograph of coalescence of fullerenes induced with electron irradiation. (A) The initial peapod; (B)–(H) consecutive images taken with an interval of 60–90 seconds during the irradiation.

Reprinted with permission from Hernández *et al.*, “Fullerene Coalescence in Nanopeapods: A Path to Novel Tubular Carbon”, *Nano Lett.* 2003 3(8), 1037 – 1042. Copyright (2003) American Chemical Society.

2.4.2 Applications of Peapods

While several applications of peapods are reproducible in laboratories, they are yet to be found or widely used in the industry. The said applications include usage of peapods in transistors (Shimada *et al.*, 2002; Yu *et al.*, 2005), solar cells (Li *et al.*, 2008) and drug delivery systems (Bianco *et al.*, 2005; Tripisciano *et al.*, 2009). There also several other possible applications such as peapod being used as photonic crystals

(He and Shen, 2006), switching memory since the position of a fullerene inside a peapod can be switched electronically (Kang and Hwang, 2004) and terahertz generator (Glukhova *et al.*, 2014).

2.4.3 Simulations of Carbon Peapods

The interest in theoretical calculations of carbon peapods was sparked by the successful experimental fabrications. In the work by Okada *et al.* (2001), the energetics and electronic structures of carbon peapod (encapsulating C_{60}) are calculated using the local-density approximation (LDA) in the density functional theory (DFT). Three different outer CNT are used in their calculations, i.e., CNT(8, 8), CNT(9, 9) and CNT(10, 10). Interpolation of the energy-radius graph shows that the estimated minimum diameter of the outer CNT encapsulating C_{60} is 12.8 Å. This agrees well with the experimental finding where the smallest peapod observed has a CNT diameter of 12.6 Å (Bandow *et al.*, 2001). There are also numerous DFT studies on hybrid/doped carbon peapods. One such example is the work by Ge *et al.* (2008). The spin interactions in carbon peapods with endohedral fullerenes ($Sc@C_{82}$) are modelled using hybrid density functional theory. It is found that the outer CNT has very little effect on the spin interactions between the fullerenes and simply act as a mechanical support for the fullerenes in questions. In another work based on DFT calculations, Zhang *et al.* (2013) investigated the electronic and transport properties of carbon peapod doped with vanadium. It is found that the dopant vanadium atoms are placed between neighbouring fullerenes along the CNT tubular direction. Due to the sandwiched vanadium atoms between the fullerenes, the electron transport of the peapod is also enhanced.

Monte Carlo (MC) studies on the separation between C_{60} and C_{70} molecules in carbon peapod is done by Verberck *et al.* (2012). Their MC simulations based on Metropolis acceptance rule is performed as NVT ensemble (Verberck *et al.*, 2009). The translational molecular degrees of freedom of the C_{60} fullerenes is found to vary between outer CNT with different diameter. In the case of diameter of outer CNT equals to 6.8 Å, the fullerenes are aligned in a single straight line. For diameter equals to 7.6 Å, the fullerenes are arranged in zig-zag configuration. The average distance between fullerenes in the carbon peapod is found to be around 10 Å.

Although not specifically on the transformation of carbon peapod into DWCNT, there are a few papers in early 2000 that describe the coalescences process between two fullerenes. Zhao *et al.* (2002) uses MD to simulate the cap to cap coalescence process which is already observed in experiments (Smith *et al.*, 1999). They have found that the polymerization between the caps can be described purely based on Stone-Wales mechanisms. However they did mention that van der Waals is not being considered in their simulations. Further work was done by Han *et al.* (2004) which showed the complete mapping of the polymerization process of two C_{60} into a C_{120} . They showed that the optimum pathway involved a sequence of 23 activated process (Stone-Wales mechanism). One of the earliest peapod to DWCNT simulation was done by Hernández *et al.* (2003) which they used it to accompany their experimental findings, particularly corrugated inner CNT which was formed in the resulting DWCNT. They used the Tersoff potential to describe the bonding among carbon atoms but did not mention about long range interactions. Shibuta and Maruyama (2006) also simulated the annealing of carbon peapod using the first generation reactive empirical bond order (REBO) potential coupled with a long range Lennard-Jones potential. They have concluded that chirality of the inner and outer

CNT have not much of effects on the interlayer separation distance (which is higher than MWCNT) and is due to the kinetic path of the coalescences. The paper by Suarez-Martinez *et al.* (2010) showed the sp^2 bonds fractions, ring statistics and radial distribution profiles of carbon peapods being annealed at different temperature. They use environment-dependent interaction potential (EDIP) to describe the short-range carbon-carbon interactions. However, van der Waals is not considered in their simulations hence the outer CNT is an artificial constrain using strain minimization.

It is not difficult to see that many of the works mentioned above ignore the long-range interactions (van der Waals) in the annealing of carbon peapod. It is assumed that the polymerizations between the inner fullerenes happened without the influence of the outer CNT. However in experiments, defected inner and outer CNT are found in the annealed/irradiated carbon peapods with Fig. 2.11 being one of them. In fact, physical events which are only made possible with the consideration of treating the outer CNT with both short- and long-range interactions are found later in Chapter 3 and Chapter 4. The said physical events include atomic exchange (Chapter 3), cross-linked defects (Chapter 3) and inter-linked defected layers (Chapter 4).

2.5 Topology of Carbon Nanostructures

The topology of carbon nanostructures can be described with Euler characteristic (László, 2005) and Gaussian curvatures (Hayashi, 2003; Hayashi, 2005). Perhaps the surprising fact is that both of them can be linked through the Gauss-Bonnet theorem given that Euler characteristic is a global topological invariant while Gaussian curvature is a curvature measure at a point. The mathematical descriptions of the

topology, curvature and surface of CNT and their relevance in this work is discussed here.

2.5.1 Euler Characteristic

Euler characteristic χ is a topological invariant number which describes the shape or structure of polyhedrons. The Euler characteristic is defined as

$$\chi = V - E + F \quad 2.6$$

where V is the number of vertices, E is the number of edges and F is the number of faces in a given polyhedron.

In the case of closed-cage carbon nanostructures, the structure is made of carbon rings in the shape of pentagons and hexagons. R_5 represents the total number of pentagon rings and R_6 represents the total number of hexagon rings. Since each carbon atoms are neighbored by 3 carbon atoms, the number of vertices, V is defined as follows,

$$V = \frac{5R_5 + 6R_6}{3} \quad 2.7$$

where the multiplier 5 and 6 represents the total atoms in pentagon ring and hexagon ring respectively. This essentially calculates the total carbon atoms of the nanostructure.

The edges, E is the total number of carbon-carbon bonds in the nanostructure and C-C bonds are always shared by two faces. Besides that, pentagon ring has 5 bonds and hexagon ring has 6 bonds thus E is defined as

$$E = \frac{5R_5 + 6R_6}{2}. \quad 2.8$$

The total faces, F of a carbon nanostructure is simply

$$F = R_5 + R_6. \quad 2.9$$

Substituting Eq. 2.7, Eq. 2.8 and Eq. 2.9 into Eq. 2.6, one can obtain the Euler characteristic for closed-cage carbon nanostructure in terms of pentagon and hexagon rings as

$$6\chi = R_5 \quad 2.10$$

Surprisingly R_6 vanished from the result. Using C_{60} in the following study case where C_{60} consists of 12 pentagon rings and 20 hexagon rings. Substituting R_5 in Eq. 2.10, the resulting Euler characteristic is equal to 2. This corresponds to the Euler characteristic of convex polyhedrons, *e.g.*, tetrahedron, cube, truncated icosahedron (C_{60}). For closed-cage carbon nanostructure ($\chi = 2$) consists of only hexagon and pentagon rings,

$$R_5 = 12 \quad 2.11$$

is obtained by substituting $\chi = 2$ in Eq. 2.10. This result indicates that one can build closed-cage carbon structures with any number of hexagon rings as long as the structures have 12 pentagons. In fact, if other fullerenes such as C_{28} , C_{36} , C_{50} , C_{72} and C_{540} are examined; all of them have exactly 12 pentagons in their structures. Another example of closed-cage carbon nanostructure with 12 pentagons is a capped carbon nanotube. In the following example (Fig. 2.12), a C_{60} molecule is split into half and a CNT (5, 5) is inserted in between them. The result is a capped CNT (5, 5) which consists of exactly 12 pentagons.

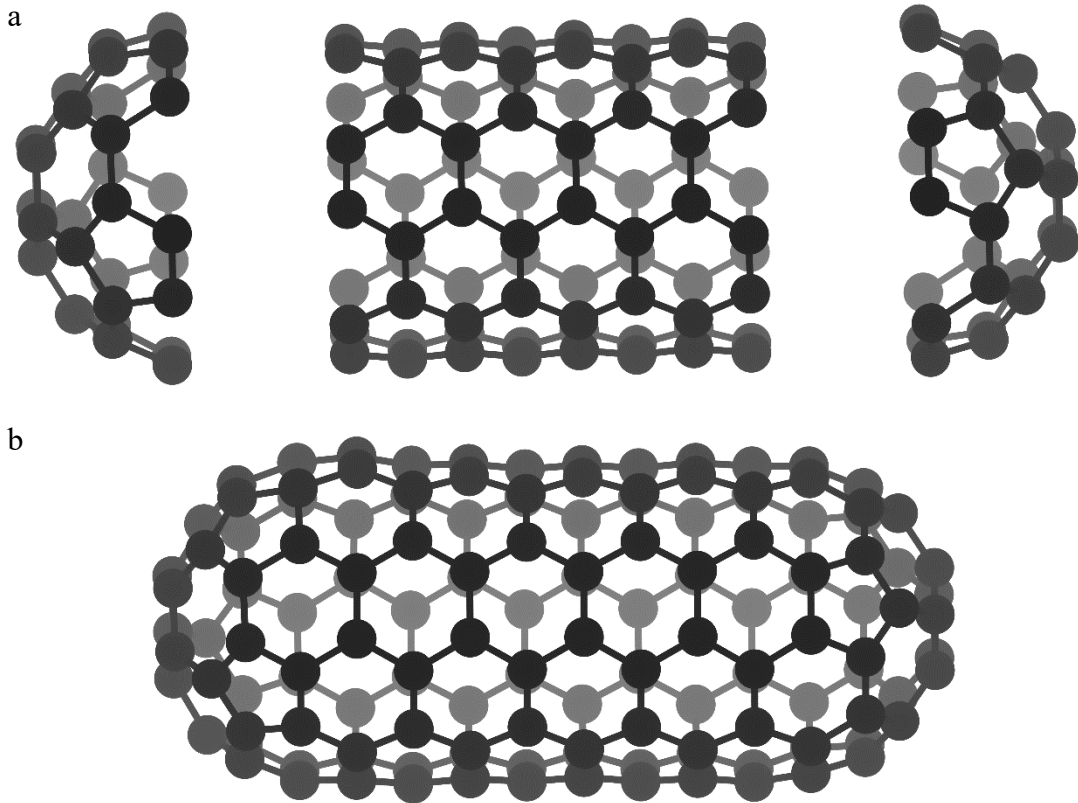


Figure 2.12: (a) Two halves of C₆₀ placed at both sides of an uncapped CNT (5, 5) (b) A capped CNT (C₁₄₀) is built by joining all three parts in (a) where exactly 12 pentagons are required to build such a closed cage structure.

However, there is one exception to this rule is that there is no structure with just one hexagon which means that there is no C₂₂. It is also energetically unfavourable for two pentagons joint to each other since it would lead to higher local curvature (when compared to joint between pentagon and hexagon). This is known as isolated pentagon rule (Kroto and McKay, 1998) where structures favour no two pentagons joined together. The smallest possible fullerene that follows isolated pentagon rule is C₆₀. This also explains why fullerenes smaller than C₆₀ are not found in soot which are used to extract fullerenes. The smallest possible structure where $R_6 = 0$ is C₂₀ which consists of pentagons only. The structure of C₂₀ molecule is also known as dodecahedral cage. C₂₀ molecule is observed through a stable C₂₀H₂₀ rather than in its

pure form (Wang *et al.*, 2001). Iqbal *et al.* 2003 also observe C₂₀ by employing ultraviolet laser ablation from diamond onto nickel substrates and obtained a face-centered-cubic (fcc) lattice with 22 carbon atoms per unit cell (C₂₀ linked with bridging carbon atoms at interstitial tetrahedral sites). Both are not direct observations of freestanding C₂₀ molecule.

The Euler characteristics can be further generalized to consider other topological variations. The Euler-Poincaré formula

$$2(1 - g) = V - E + F \quad 2.12$$

where the genus, g for closed-cage structure is 0. Structures with hole such as carbon nanotorus are categorized as genus, $g = 1$; structures with two holes are genus-two surface ($g = 2$) and so on. One can change the form of the Euler-Poincaré formula by considering polygons (triangle, square, heptagon, octagon and so on) instead of vertices, edges and faces. This is relevant in carbon nanostructure as defects such as heptagon rings and octagon rings are observed in carbon nanotubes and graphene (Ugeda *et al.*, 2012). In this work, the total rings of each type will be calculated and plotted on graph which will then reveal the details of the carbon nanostructure. Another reason for using rings instead of vertices, edges and faces is due to Gaussian curvatures that can be explained much easier using rings. Here the relations between the summation of rings and each of the original variables, E , V and F extending from Eq. 2.7, Eq. 2.8 and Eq. 2.9 are defined as follows.